

# Two-loop additive mass renormalization with clover fermions and Symanzik improved gluons

A. Skouroupathis,\* M. Constantinou,<sup>†</sup> and H. Panagopoulos<sup>‡</sup>

*Department of Physics, University of Cyprus, P.O. Box 20537, Nicosia CY-1678, Cyprus*

(Received 22 October 2007; published 25 January 2008)

We calculate the critical value of the hopping parameter,  $\kappa_c$ , in lattice QCD, up to two loops in perturbation theory. We employ the Sheikholeslami-Wohlert (clover) improved action for fermions and the Symanzik improved gluon action with 4- and 6-link loops. The quantity which we study is a typical case of a vacuum expectation value resulting in an additive renormalization; as such, it is characterized by a power (linear) divergence in the lattice spacing, and its calculation lies at the limits of applicability of perturbation theory. Our results are polynomial in  $c_{\text{SW}}$  (clover parameter) and cover a wide range of values for the Symanzik coefficients  $c_i$ . The dependence on the number of colors  $N$  and the number of fermion flavors  $N_f$  is shown explicitly. In order to compare our results to nonperturbative evaluations of  $\kappa_c$  coming from Monte Carlo simulations, we employ an improved perturbation theory method for improved actions.

DOI: 10.1103/PhysRevD.77.014513

PACS numbers: 11.15.Ha, 11.10.Gh, 12.38.Bx, 12.38.Gc

## I. INTRODUCTION

In the present work, we calculate the additive renormalization of the fermion mass in lattice QCD, using clover fermions and Symanzik improved gluons. The calculation is carried out up to two loops in perturbation theory and it is directly related to the determination of the critical value of the hopping parameter,  $\kappa_c$ .

The clover fermion action [1] (SW) successfully reduces lattice discretization effects and approaches the continuum limit faster. This justifies the extensive usage of this action in Monte Carlo simulations in recent years. The coefficient  $c_{\text{SW}}$  appearing in this action is a free parameter for the current work and our results will be given as a polynomial in  $c_{\text{SW}}$ .

Regarding gluon fields, we employ the Symanzik improved action [2], which also aims at minimizing finite lattice spacing effects. For the coefficients parametrizing the Symanzik action, we consider several choices of values which are frequently used in the literature.

The lattice discretization of fermions introduces some well-known difficulties; demanding strict locality and absence of doublers leads to the breaking of chiral symmetry. In order to recover this symmetry in the continuum limit one must set the renormalized fermion mass ( $m_R$ ) equal to zero. To achieve this, the mass parameter  $m_\circ$  appearing in the Lagrangian must approach a critical value  $m_c$ , which is nonzero due to additive renormalization.

The mass parameter  $m_\circ$  is directly related to the hopping parameter  $\kappa$  used in simulations. Its critical value,  $\kappa_c$ , corresponds to chiral symmetry restoration:

$$\kappa_c = \frac{1}{2m_c a + 8r}, \quad (1)$$

where  $a$  is the lattice spacing and  $r$  is the Wilson parameter.

Using Eq. (1), the nonrenormalized fermion mass is given by

$$m_B \equiv m_\circ - m_c = \frac{1}{2a} \left( \frac{1}{\kappa} - \frac{1}{\kappa_c} \right). \quad (2)$$

Thus, in order to restore chiral symmetry one must consider the limit  $m_\circ \rightarrow m_c$ . This fact points to the necessity of an evaluation of  $m_c$ .

The perturbative value of  $m_c$  is also a necessary ingredient in higher-loop calculations of the multiplicative renormalization of operators (see, e.g., Ref. [3]). In mass independent schemes, such renormalizations are typically defined and calculated at zero renormalized mass, and this entails setting the value of the Lagrangian mass equal to  $m_c$ .

Previous studies of the hopping parameter and its critical value have appeared in the literature for Wilson fermions-Wilson gluons [4] and for clover fermions-Wilson gluons [5,6]. The procedure and notation in our work is the same as in the above references.

Our results for  $\kappa_c$  (and consequently for the critical fermion mass) depend on the number of colors ( $N$ ) and on the number of fermion flavors ( $N_f$ ). Besides that, there is an explicit dependence on the clover parameter  $c_{\text{SW}}$  which, as mentioned at the beginning, is kept as a free parameter. On the other hand, the dependence of the results on the choice of Symanzik coefficients cannot be given in closed form; instead, we present it in a list of tables and figures.

The rest of the paper is organized as follows: In Sec. II we formulate the problem, define the discretized actions, and describe our calculation of the necessary Feynman diagrams. Section III is a presentation of our results. Finally, in Sec. IV we apply to our one- and two-loop results an improvement method, proposed by us [7–9]. This method resums a certain infinite class of subdiagrams, to all orders in perturbation theory, leading to an improved perturbative expansion. We end this section with a com-

\*php4as01@ucy.ac.cy

<sup>†</sup>phpgmc1@ucy.ac.cy

<sup>‡</sup>haris@ucy.ac.cy

parison of perturbative and nonperturbative results. Our findings are summarized in Sec. V.

## II. FORMULATION OF THE PROBLEM

We begin with the Wilson formulation of the QCD action on the lattice, with  $N_f$  flavors of degenerate clover (SW) [1] fermions. In standard notation, it reads:

$$\begin{aligned} S_L = S_G + \sum_f \sum_x (4r + m_*) \bar{\psi}_f(x) \psi_f(x) \\ - \frac{1}{2} \sum_f \sum_{x,\mu} [\bar{\psi}_f(x)(r - \gamma_\mu) U_{x,x+\mu} \psi_f(x+\mu) \\ + \bar{\psi}_f(x+\mu)(r + \gamma_\mu) U_{x+\mu,x} \psi_f(x)] \\ + \frac{i}{4} c_{\text{SW}} \sum_f \sum_{x,\mu,\nu} \bar{\psi}_f(x) \sigma_{\mu\nu} \hat{F}_{\mu\nu}(x) \psi_f(x), \end{aligned} \quad (3)$$

$$\text{where: } \hat{F}_{\mu\nu} \equiv \frac{1}{8}(Q_{\mu\nu} - Q_{\nu\mu}) \quad (4)$$

$$\begin{aligned} \text{and: } Q_{\mu\nu} = U_{x,x+\mu} U_{x+\mu,x+\mu+\nu} U_{x+\mu+\nu,x+\nu} U_{x+\nu,x} \\ + U_{x,x+\nu} U_{x+\nu,x+\nu-\mu} U_{x+\nu-\mu,x-\mu} U_{x-\mu,x} \\ + U_{x,x-\mu} U_{x-\mu,x-\mu-\nu} U_{x-\mu-\nu,x-\nu} U_{x-\nu,x} \\ + U_{x,x-\nu} U_{x-\nu,x-\nu+\mu} U_{x-\nu+\mu,x+\mu} U_{x+\mu,x}. \end{aligned} \quad (5)$$

The clover coefficient  $c_{\text{SW}}$  is treated here as a free parameter. Particular choices of values for  $c_{\text{SW}}$  have been determined both perturbatively [1] and nonperturbatively [10], so as to minimize  $\mathcal{O}(a)$  effects. The Wilson parameter  $r$  is set to  $r = 1$  henceforth;  $f$  is a flavor index;  $\sigma_{\mu\nu} = (i/2)[\gamma_\mu, \gamma_\nu]$ . Powers of the lattice spacing  $a$  have been omitted and may be directly reinserted by dimensional counting.

Regarding gluons, we use the Symanzik improved gauge field action, involving Wilson loops with 4 and 6 links<sup>1</sup>:

$$\begin{aligned} S_G = \frac{2}{g^2} \left[ c_0 \sum_{\text{plaquette}} \text{Re Tr}\{1 - U_{\text{plaquette}}\} \right. \\ + c_1 \sum_{\text{rectangle}} \text{Re Tr}\{1 - U_{\text{rectangle}}\} \\ + c_2 \sum_{\text{chair}} \text{Re Tr}\{1 - U_{\text{chair}}\} \\ \left. + c_3 \sum_{\text{parallelogram}} \text{Re Tr}\{1 - U_{\text{parallelogram}}\} \right] \quad (6) \end{aligned}$$

( $g$  is the bare coupling constant). The lowest order expansion of this action, leading to the gluon propagator, is

<sup>1</sup>1 × 1 plaquette, 1 × 2 rectangle, 1 × 2 chair (bent rectangle), and 1 × 1 × 1 parallelogram wrapped around an elementary 3d cube.

$$\begin{aligned} S_G^{(0)} = \frac{1}{2} \int_{-\pi/a}^{\pi/a} \frac{d^4 k}{(2\pi)^4} \sum_{\mu\nu} A_\mu^a(k) \left[ G_{\mu\nu}(k) - \frac{\xi}{\xi - 1} \hat{k}_\mu \hat{k}_\nu \right] \\ \times A_\nu^a(-k), \end{aligned} \quad (7)$$

where  $\xi$  is the gauge-fixing parameter (see Eq. (10)) and

$$\begin{aligned} G_{\mu\nu}(k) &= \hat{k}_\mu \hat{k}_\nu + \sum_\rho (\hat{k}_\rho^2 \delta_{\mu\nu} - \hat{k}_\mu \hat{k}_\rho \delta_{\mu\nu}) d_{\mu\rho}, \\ \hat{k}_\mu &= \frac{2}{a} \sin \frac{ak_\mu}{2}, \quad \hat{k}^2 = \sum_\mu \hat{k}_\mu^2, \end{aligned} \quad (8)$$

$$d_{\mu\nu} = (1 - \delta_{\mu\nu}) [C_0 - C_1 a^2 \hat{k}^2 - C_2 a^2 (\hat{k}_\mu^2 + \hat{k}_\nu^2)].$$

The coefficients  $C_i$  are related to  $c_i$  by

$$\begin{aligned} C_0 &= c_0 + 8c_1 + 16c_2 + 8c_3, & C_1 &= c_2 + c_3, \\ C_2 &= c_1 - c_2 - c_3. \end{aligned} \quad (9)$$

The Symanzik coefficients must satisfy:  $c_0 + 8c_1 + 16c_2 + 8c_3 = 1$ , in order to reach the correct classical continuum limit. Aside from this requirement, the values of  $c_i$  can be chosen arbitrarily; they are normally tuned in a way as to ensure  $\mathcal{O}(a)$  improvement.

As always in perturbation theory, we must introduce an appropriate gauge-fixing term to the action; in terms of the gauge field  $Q_\mu(x)$  [ $U_{x,x+\mu} = \exp(igQ_\mu(x))$ ], it reads:

$$\begin{aligned} S_{\text{gf}} &= \frac{1}{1 - \xi} \sum_{x,\mu,\nu} \text{Tr}\{\Delta_\mu^- Q_\mu(x) \Delta_\nu^- Q_\nu(x)\}, \\ \Delta_\mu^- Q_\nu(x) &\equiv Q_\nu(x - \hat{\mu}) - Q_\nu(x). \end{aligned} \quad (10)$$

Having to compute a gauge invariant quantity, we can, for convenience, choose to work either in the Feynman gauge ( $\xi = 0$ ) or in the Landau gauge ( $\xi = 1$ ). Covariant gauge-fixing produces the following action for the ghost fields  $\omega$  and  $\bar{\omega}$

$$\begin{aligned} S_{\text{gh}} = 2 \sum_x \sum_\mu \text{Tr} \Bigl\{ &(\Delta_\mu^+ \omega(x))^\dagger \\ &\times \left( \Delta_\mu^+ \omega(x) + ig [Q_\mu(x), \omega(x)] \right. \\ &+ \frac{1}{2} ig [Q_\mu(x), \Delta_\mu^+ \omega(x)] \\ &\left. - \frac{1}{12} g^2 [Q_\mu(x), [Q_\mu(x), \Delta_\mu^+ \omega(x)]] + \dots \right) \Bigr\}, \\ \Delta_\mu^+ \omega(x) &\equiv \omega(x + \hat{\mu}) - \omega(x). \end{aligned} \quad (11)$$

Finally, the change of integration variables from links to vector fields yields a Jacobian that can be rewritten as the usual measure term  $S_m$  in the action:

$$S_m = \frac{1}{12} N g^2 \sum_x \sum_\mu \text{Tr}\{Q_\mu(x) Q_\mu(x)\} + \dots \quad (12)$$

In  $S_{\text{gh}}$  and  $S_m$  we have written out only terms relevant to

our computation. The full action is:  $S = S_L + S_{\text{gf}} + S_{\text{gh}} + S_m$ .

The bare fermion mass  $m_B$  must be set to zero for chiral invariance in the classical continuum limit. Terms proportional to  $r$  in the action, as well as the clover terms, break chiral invariance. They vanish in the classical continuum limit; at the quantum level, they induce nonvanishing, flavor-independent fermion mass corrections. Numerical simulation algorithms usually employ the hopping parameter

$$\kappa \equiv \frac{1}{2m_\circ a + 8r} \quad (13)$$

as an adjustable input. Its critical value, at which chiral symmetry is restored, is thus  $1/8r$  classically, but gets shifted by quantum effects.

The renormalized mass can be calculated in textbook fashion from the fermion self-energy. Denoting by  $\Sigma^L(p, m_\circ, g)$  the truncated, one particle irreducible fermion two-point function, we have for the fermion propagator:

$$S(p) = [i\overset{\circ}{p} + m(p) - \Sigma^L(p, m_\circ, g)]^{-1},$$

where:  $\overset{\circ}{p} = \frac{1}{a} \sum_\mu \gamma_\mu \sin(ap^\mu)$ ,  $m(p) = m_\circ + \frac{2r}{a} \sum_\mu \sin^2(ap^\mu/2)$ . (14)

To restore the explicit breaking of chiral invariance, we require that the renormalized mass vanish:

$$S^{-1}(0)|_{m_\circ \rightarrow m_c} = 0 \Rightarrow m_c = \Sigma^L(0, m_c, g). \quad (15)$$

The above is a recursive equation for  $m_c$ , which can be solved order by order in perturbation theory.

We denote by  $dm$  the additive mass renormalization of  $m_\circ$ :  $m_B = m_\circ - dm$ . In order to obtain a zero renormalized mass, we must require  $m_B \rightarrow 0$ , and thus  $m_\circ \rightarrow dm$ . Consequently,

$$m_c = dm = dm_{(1\text{-loop})} + dm_{(2\text{-loop})}. \quad (16)$$

At tree level,  $m_c = 0$ .

Two diagrams contribute to  $dm_{(1\text{-loop})}$ , shown in Fig. 1. In these diagrams, the fermion mass must be set to its tree-level value,  $m_\circ \rightarrow 0$ .

The quantity  $dm_{(2\text{-loop})}$  receives contributions from a total of 26 diagrams, shown in Fig. 2. Genuine two-loop



FIG. 1. One-loop diagrams contributing to  $dm_{(1\text{-loop})}$ . Wavy (solid) lines represent gluons (fermions).

diagrams must again be evaluated at  $m_\circ \rightarrow 0$ ; in addition, one must include to this order the one-loop diagram containing an  $\mathcal{O}(g^2)$  mass counterterm (diagram 23).

Certain sets of diagrams, corresponding to one-loop renormalization of propagators, must be evaluated together in order to obtain an infrared convergent result: These are diagrams  $7 + 8 + 9 + 10 + 11, 12 + 13, 14 + 15 + 16 + 17 + 18, 19 + 20, 21 + 22 + 23$ .

### III. COMPUTATION AND RESULTS

Given that the dependence of  $m_c$  on the Symanzik coefficients  $c_i$  cannot be expressed in closed form, we chose certain sets of values for  $c_i$ , presented in Table I, which are in common use [11–16]: Plaquette, Symanzik (tree-level improved), Tadpole Improved Lüscher-Weisz (TILW), Iwasaki and DBW2. Actually, since the gluon propagator contains only the combinations  $C_1$  and  $C_2$  (Eq. (9)), all results for  $m_c$  can be recast in terms of  $C_1, C_2$  and one additional parameter, say,  $c_2$ ; in this case the dependence on  $c_2$  (at fixed  $C_1, C_2$ ) is a polynomial of second degree.

The contribution  $dm_l$  of the  $l^{\text{th}}$  one-loop diagram to  $dm$ , can be expressed as

$$dm_l = \frac{(N^2 - 1)}{N} g^2 \cdot \sum_{i=0}^2 c_{\text{SW}}^i \varepsilon_l^{(i)}, \quad (17)$$

where  $\varepsilon_l^{(i)}$  are numerical one-loop integrals whose values depend on  $C_1, C_2$ . The dependence on  $c_{\text{SW}}$  is seen to be a polynomial of degree 2 ( $i = 0, 1, 2$ ).

The contribution to  $dm$  from two-loop diagrams that do not contain closed fermion loops, can be written in the form

$$dm_l = \frac{(N^2 - 1)}{N^2} g^4 \cdot \sum_{i,j,k} c_{\text{SW}}^i N^j c_2^k e_l^{(i,j,k)}, \quad (18)$$

where the index  $l$  runs over all contributing diagrams,  $j = 0, 2$  and  $k = 0, 1, 2$  (since up to two vertices from the gluon action may be present in a Feynman diagram). The dependence on  $c_{\text{SW}}$  is now a polynomial of degree 4 ( $i = 0, \dots, 4$ ). The coefficients  $e_l^{(i,j,k)}$  (as well as  $\tilde{e}_l^{(i)}$  of Eq. (19) below) are two-loop numerical integrals; once again, they depend on  $C_1, C_2$ . Finally, the contribution to  $dm$  from two-loop diagrams containing a closed fermion loop, can be expressed as

$$dm_l = \frac{(N^2 - 1)}{N} N_f g^4 \cdot \sum_{i=0}^4 c_{\text{SW}}^i \tilde{e}_l^{(i)}, \quad (19)$$

where the index  $l$  runs over diagrams 12–13, 19–20. Summing up the contributions of all diagrams,  $dm$  assumes the form

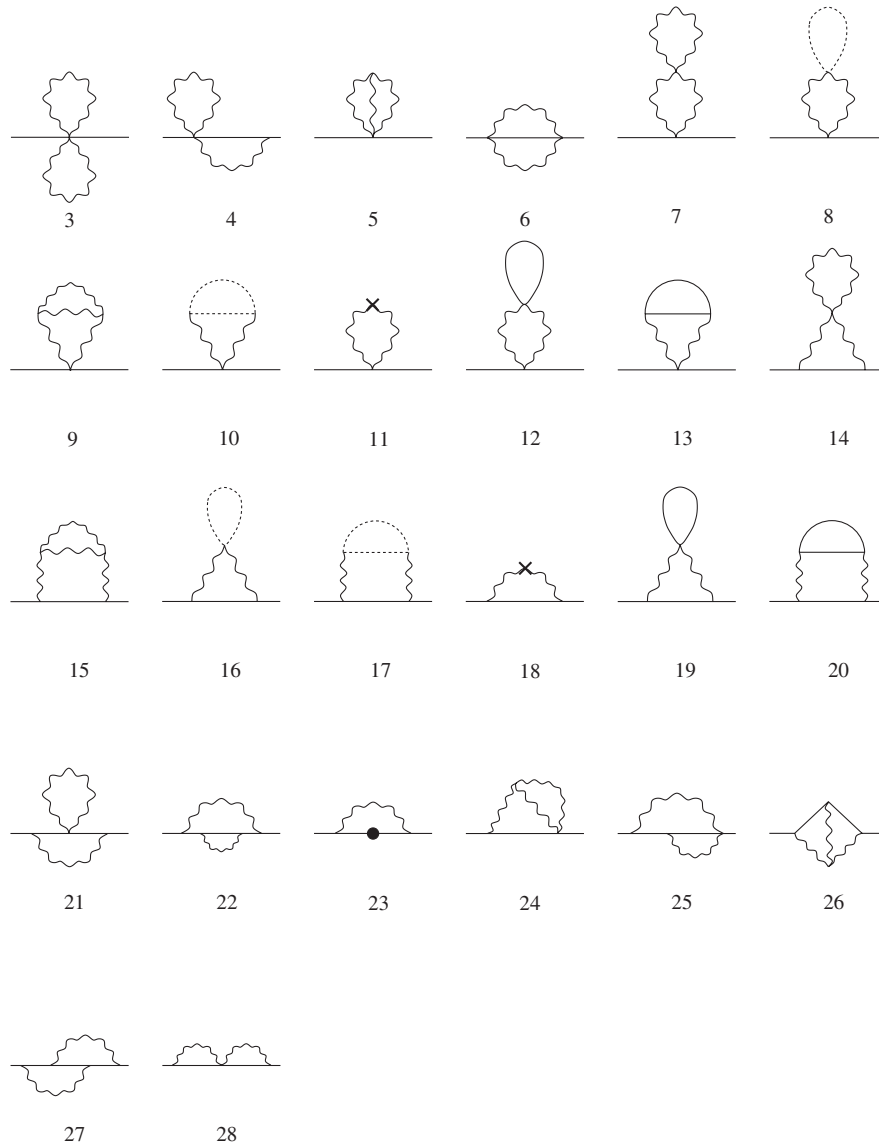


FIG. 2. Two-loop diagrams contributing to  $dm_{(2\text{-loop})}$ . Wavy (solid, dotted) lines represent gluons (fermions, ghosts). Crosses denote vertices stemming from the measure part of the action; a solid circle is a fermion mass counterterm.

$$\begin{aligned}
 dm &= \sum_l dm_l \\
 &= \frac{(N^2 - 1)}{N} g^2 \cdot \sum_i c_{SW}^i \epsilon^{(i)} + \frac{(N^2 - 1)}{N^2} g^4 \\
 &\quad \cdot \sum_{i,j,k} c_{SW}^i N^j c_2^k e^{(i,j,k)} + \frac{(N^2 - 1)}{N} N_f g^4 \cdot \sum_i c_{SW}^i \tilde{e}^{(i)}. \tag{20}
 \end{aligned}$$

In the above,  $\epsilon^{(i)}$ ,  $e^{(i,j,k)}$ ,  $\tilde{e}^{(i)}$  are the sums over all contributing diagrams of the quantities:  $\epsilon_l^{(i)}$ ,  $e_l^{(i,j,k)}$ ,  $\tilde{e}_l^{(i)}$ , respectively, (cf. Eqs. (17)–(19)).

TABLE I. Input parameters  $c_0$ ,  $c_1$ ,  $c_3$  ( $c_2 = 0$ ).

Action	$c_0$	$c_1$	$c_3$
Plaquette	1.0	0	0
Symanzik	1.666 666 7	-0.083 333	0
TILW, $\beta c_0 = 8.60$	2.316 806 4	-0.151 791	-0.012 809 8
TILW, $\beta c_0 = 8.45$	2.346 024 0	-0.154 846	-0.013 407 0
TILW, $\beta c_0 = 8.30$	2.386 977 6	-0.159 128	-0.014 244 2
TILW, $\beta c_0 = 8.20$	2.412 784 0	-0.161 827	-0.014 771 0
TILW, $\beta c_0 = 8.10$	2.446 540 0	-0.165 353	-0.015 464 5
TILW, $\beta c_0 = 8.00$	2.489 171 2	-0.169 805	-0.016 341 4
Iwasaki	3.648	-0.331	0
DBW2	12.2688	-1.4086	0

The coefficients  $\varepsilon^{(i)}$  lead to the total contribution of one-loop diagrams. Their values are listed in Table II, for the ten sets of  $c_i$  values shown in Table I. Similarly, results for the coefficients  $e^{(i,j,k)}$  and  $\tilde{e}^{(i)}$  corresponding to the total contribution of two-loop diagrams, are presented in Tables III, IV, V, VI, and VII.

In order to enable cross-checks and comparisons, numerical per-diagram values of the constants  $\varepsilon_l^{(i)}$ ,  $e_l^{(i,j,k)}$ , and  $\tilde{e}_l^{(i)}$  are presented in Tables VIII, IX, X, XI, and XII,

for the case of the Iwasaki action. For economy of space, several vanishing contributions to these constants have simply been omitted. A similar breakdown for other actions can be obtained from the authors upon request.

The total contribution of one-loop diagrams, for  $N = 3$ , can be written as a function of the clover parameter  $c_{\text{SW}}$ . In the case of the Plaquette, Iwasaki, and DBW2 actions, we find, respectively:

TABLE II. Total contribution of one-loop diagrams.

Action	$\varepsilon^{(0)}$	$\varepsilon^{(1)}$	$\varepsilon^{(2)}$
Plaquette	-0.162 857 058 2(5)	0.043 483 033 9(1)	0.018 095 768 75(4)
Symanzik	-0.128 054 905 28(8)	0.037 831 493 1(2)	0.014 763 358 01(5)
TILW (8.60)	-0.108 215 687 68(4)	0.034 085 602 32(6)	0.012 659 919 72(4)
TILW (8.45)	-0.107 491 856 25(3)	0.033 940 937 5(1)	0.012 581 088 95(1)
TILW (8.30)	-0.106 496 287 2(3)	0.033 740 986 9(2)	0.012 472 434 543(4)
TILW (8.20)	-0.105 879 983 1(2)	0.033 616 637 2(1)	0.012 405 041 6(1)
TILW (8.10)	-0.105 086 619 1(1)	0.033 455 916 21(5)	0.012 318 127 134(5)
TILW (8.00)	-0.104 104 478 93(3)	0.033 255 936 31(8)	0.012 210 297 749(7)
Iwasaki	-0.082 554 356 13(4)	0.028 545 138 7(1)	0.009 834 908 67(5)
DBW2	-0.036 452 662 3(2)	0.015 816 574 12(5)	0.004 280 099 253(2)

TABLE III. Total contribution of two-loop diagrams of order  $\mathcal{O}(N^2, c_2^0)$ .

Action	$e^{(0,2,0)}$	$e^{(1,2,0)}$	$e^{(2,2,0)}$	$e^{(3,2,0)}$	$e^{(4,2,0)}$
Plaquette	-0.017 536 02(2)	0.002 599 63(2)	-0.000 155 894(8)	-0.000 163 242(2)	-0.000 017 217 59(2)
Symanzik	-0.008 103 66(1)	0.000 950 46(2)	-0.000 404 510(9)	-0.000 107 348(2)	-0.000 012 759 04(1)
TILW (8.60)	-0.004 370 13(7)	0.000 194 03(5)	-0.000 458 94(1)	-0.000 078 117(3)	-0.000 010 208 20(1)
TILW (8.45)	-0.004 255 75(7)	0.000 169 78(6)	-0.000 459 62(1)	-0.000 077 102(3)	-0.000 010 114 51(1)
TILW (8.30)	-0.004 100 86(7)	0.000 136 82(7)	-0.000 460 40(1)	-0.000 075 713(3)	-0.000 009 985 64(1)
TILW (8.20)	-0.004 006 36(6)	0.000 116 66(8)	-0.000 460 80(1)	-0.000 074 857(3)	-0.000 009 905 84(1)
TILW (8.10)	-0.003 886 30(6)	0.000 090 97(9)	-0.000 461 23(1)	-0.000 073 760(3)	-0.000 009 803 14(1)
TILW (8.00)	-0.003 740 09(6)	0.000 059 58(9)	-0.000 461 601(9)	-0.000 072 410(3)	-0.000 009 676 00(1)
Iwasaki	-0.001 129 57(2)	-0.000 529 64(6)	-0.000 436 966(5)	-0.000 045 009(3)	-0.000 006 823 53(1)
DBW2	0.000 848 1(2)	-0.000 853 01(8)	-0.000 185 40(1)	-0.000 006 164(3)	-0.000 001 735 02(3)

TABLE IV. Total contribution of two-loop diagrams of order  $\mathcal{O}(N^0, c_2^0)$ .

Action	$e^{(0,0,0)}$	$e^{(1,0,0)}$	$e^{(2,0,0)}$	$e^{(3,0,0)}$	$e^{(4,0,0)}$
Plaquette	0.016 566 33(2)	-0.000 559 04(1)	0.002 622 771(7)	0.000 158 125(2)	0.000 042 826 74(2)
Symanzik	0.006 056 56(1)	0.000 935 801(6)	0.002 120 980(9)	0.000 104 973(2)	0.000 029 715 53(1)
TILW (8.60)	0.002 026 37(3)	0.001 578 90(3)	0.001 790 242(9)	0.000 076 167(2)	0.000 022 606 69(1)
TILW (8.45)	0.001 907 29(3)	0.001 598 00(3)	0.001 777 415(9)	0.000 075 164(3)	0.000 022 356 03(1)
TILW (8.30)	0.001 746 66(3)	0.001 623 75(2)	0.001 759 689(9)	0.000 073 791(3)	0.000 022 012 43(1)
TILW (8.20)	0.001 649 01(3)	0.001 639 39(2)	0.001 748 661(9)	0.000 072 944(3)	0.000 021 800 41(1)
TILW (8.10)	0.001 525 32(3)	0.001 659 17(2)	0.001 734 421(9)	0.000 071 859(3)	0.000 021 528 26(1)
TILW (8.00)	0.001 375 35(4)	0.001 683 10(3)	0.001 716 71(1)	0.000 070 522(3)	0.000 021 192 59(1)
Iwasaki	-0.001 030 22(1)	0.002 032 54(1)	0.001 313 076(3)	0.000 043 949(3)	0.000 014 233 24(1)
DBW2	-0.001 896 1(2)	0.001 613 0(3)	0.000 413 397(9)	0.000 005 057(3)	0.000 003 074 80(3)

TABLE V. Total contribution of two-loop diagrams containing closed fermion loops.

Action	$\tilde{e}^{(0)}$	$\tilde{e}^{(1)}$	$\tilde{e}^{(2)}$	$\tilde{e}^{(3)}$	$\tilde{e}^{(4)}$
Plaquette	0.001 186 21(2)	-0.000 546 197(8)	0.001 365 146(9)	-0.000 692 228(3)	-0.000 198 097 91(7)
Symanzik	0.000 814 96(1)	-0.000 448 276(6)	0.001 041 379(8)	-0.000 574 521(3)	-0.000 145 337 0(2)
TILW (8.60)	0.000 636 43(1)	-0.000 389 464(5)	0.000 857 737(3)	-0.000 500 011(5)	-0.000 114 849 1(1)
TILW (8.45)	0.000 630 33(1)	-0.000 387 269(5)	0.000 851 127(3)	-0.000 497 194(5)	-0.000 113 754 4(1)
TILW (8.30)	0.000 621 98(1)	-0.000 384 243(5)	0.000 842 047(3)	-0.000 493 307(5)	-0.000 112 251 5(1)
TILW (8.20)	0.000 616 84(1)	-0.000 382 366(5)	0.000 836 433(3)	-0.000 490 894(5)	-0.000 111 322 7(1)
TILW (8.10)	0.000 610 25(1)	-0.000 379 946(5)	0.000 829 214(4)	-0.000 487 781(4)	-0.000 110 128 8(1)
TILW (8.00)	0.000 602 14(1)	-0.000 376 945(5)	0.000 820 289(4)	-0.000 483 915(4)	-0.000 108 653 6(1)
Iwasaki	0.000 435 46(1)	-0.000 308 00(1)	0.000 629 274(8)	-0.000 395 294(3)	-0.000 077 953 8(3)
DBW2	0.000 158 33(3)	-0.000 148 83(4)	0.000 247 56(2)	-0.000 182 42(5)	-0.000 021 359 5(6)

TABLE VI. Total contribution of two-loop diagrams containing the parameter  $c_2$  (part 1).

Action	$e^{(0,0,1)}$	$e^{(1,0,1)}$	$e^{(2,0,1)}$	$e^{(0,2,1)}$	$e^{(1,2,1)}$
Plaquette	0.077 167(3)	-0.019 808(3)	-0.008 541 5(2)	-0.047 102(4)	0.010 439(3)
Symanzik	0.034 929(2)	-0.010 895(2)	-0.004 145 4(2)	-0.017 940(2)	0.004 491(2)
TILW (8.60)	0.020 247(1)	-0.007 117(2)	-0.002 455 9(1)	-0.008 702(1)	0.002 251(1)
TILW (8.45)	0.019 816(1)	-0.006 998(2)	-0.002 405 0(1)	-0.008 448(1)	0.002 185(1)
TILW (8.30)	0.019 235(1)	-0.006 835(2)	-0.002 336 2(1)	-0.008 107 8(6)	0.002 097 3(9)
TILW (8.20)	0.018 881(1)	-0.006 736(2)	-0.002 294 2(1)	-0.007 902 3(7)	0.002 044(1)
TILW (8.10)	0.018 433(1)	-0.006 609(2)	-0.002 241 0(1)	-0.007 643 1(9)	0.001 976 1(8)
TILW (8.00)	0.017 888(1)	-0.006 454(2)	-0.002 176 2(1)	-0.007 330 0(6)	0.001 894 0(6)
Iwasaki	0.008 761 5(7)	-0.003 656(1)	-0.001 078 56(8)	-0.002 748 4(4)	0.000 664 6(5)
DBW2	0.000 790 7(2)	-0.000 488 9(3)	-0.000 083 43(2)	0.000 130 8(2)	-0.000 158 7(3)

TABLE VII. Total contribution of two-loop diagrams containing the parameter  $c_2$  (part 2).

Action	$e^{(2,2,1)}$	$e^{(3,2,1)}$	$e^{(0,2,2)}$	$e^{(1,2,2)}$	$e^{(2,2,2)}$
Plaquette	0.003 924 5(3)	-0.000 084 214 3(1)	-0.094 482 52(9)	0.027 559 93(3)	0.010 521 016(1)
Symanzik	0.001 462 2(1)	-0.000 045 498 6(1)	-0.034 175 49(2)	0.012 489 53(1)	0.004 104 789 1(2)
TILW (8.60)	0.000 647 2(1)	-0.000 028 723 41(6)	-0.017 374 635(6)	0.007 205 477(3)	0.002 121 844 3(2)
TILW (8.45)	0.000 625 1(1)	-0.000 028 181 23(6)	-0.016 917 713(6)	0.007 049 188(2)	0.002 066 619 2(2)
TILW (8.30)	0.000 595 4(1)	-0.000 027 443 85(5)	-0.016 304 614(5)	0.006 838 088(3)	0.001 992 404 7(3)
TILW (8.20)	0.000 577 5(1)	-0.000 026 992 23(5)	-0.015 933 835(5)	0.006 709 626(4)	0.001 947 460 4(2)
TILW (8.10)	0.000 555 0(1)	-0.000 026 416 46(5)	-0.015 466 270(5)	0.006 546 741(4)	0.001 890 712 1(3)
TILW (8.00)	0.000 527 9(1)	-0.000 025 712 31(5)	-0.014 902 324(4)	0.006 348 924(5)	0.001 822 164 3(3)
Iwasaki	0.000 157 19(6)	-0.000 012 492 81(2)	-0.005 961 23(2)	0.002 955 02(1)	0.000 728 681 6(4)
DBW2	-0.000 024 36(1)	-0.000 000 504 04(9)	-0.000 287 31(2)	0.000 203 17(4)	0.000 027 881 0(8)

TABLE VIII. Contribution of one-loop diagrams, for the Iwasaki action.

$i$	$\varepsilon_1^{(i)}$	$\varepsilon_2^{(i)}$
0	-0.056 026 368 32(2)	-0.026 527 987 81(3)
1	0	0.028 545 138 7(1)
2	0	0.009 834 908 67(5)

$$dm_{(1\text{-loop})}^{\text{Plaquette}} = g^2(-0.434 285 489(1) + 0.115 954 757 0(3)c_{\text{SW}} + 0.048 255 383 3(1)c_{\text{SW}}^2), \quad (21)$$

$$dm_{(1\text{-loop})}^{\text{Iwasaki}} = g^2(-0.220 144 949 7(1) + 0.076 120 369 8(3)c_{\text{SW}} + 0.026 226 423 1(1)c_{\text{SW}}^2), \quad (22)$$

$$dm_{(1\text{-loop})}^{\text{DBW2}} = g^2(-0.097 207 099 5(5) + 0.042 177 531 0(1)c_{\text{SW}} + 0.011 413 598 01(1)c_{\text{SW}}^2). \quad (23)$$

TABLE IX. Contribution of diagrams 3, 4, 6, for the Iwasaki action.

$i$	$j$	$k$	$e_3^{(i,j,k)}$	$e_4^{(i,j,k)}$	$e_6^{(i,j,k)}$
0	0	0	-0.000 392 368 6(9)	-0.000 743 134(3)	-0.000 071 488 2(8)
0	2	0	0.000 261 579 1(6)	0.000 495 422(2)	0.000 035 744 1(4)
1	0	0	0	0.001 900 337(2)	0
1	2	0	0	0.001 777 441 0(9)	0
2	0	0	0	-0.001 033 972 0(2)	0
2	2	0	0	-0.001 041 123(1)	0.000 279 923 8(4)

TABLE X. Contribution of diagrams 7–11, 14–18, 24, 26, for the Iwasaki action.

$i$	$j$	$k$	$e_{7-11}^{(i,j,k)}$	$e_{14-18}^{(i,j,k)}$	$e_{24}^{(i,j,k)}$	$e_{26}^{(i,j,k)}$
0	0	0	0.000 428 02(1)	-0.000 195 263(2)	0	0
0	0	1	0.005 710 3(7)	0.003 051 2(2)	0	0
0	2	0	-0.001 119 95(2)	-0.000 297 48(1)	0	-0.000 298 742(2)
0	2	1	-0.002 247 2(3)	-0.000 871 8(2)	0	0.000 370 589 3(7)
0	2	2	-0.003 712 63(2)	-0.002 248 59(1)	0	0
1	0	0	0	0.000 645 34(1)	0	0
1	0	1	0	-0.003 656(1)	0	0
1	2	0	0	0.000 110 79(6)	-0.000 144 897(2)	0.000 429 899(1)
1	2	1	0	0.000 645 0(5)	0.000 248 682(4)	-0.000 229 05(1)
1	2	2	0	0.002 955 02(1)	0	0
2	0	0	0	-0.000 000 974(1)	0	0
2	0	1	0	-0.001 078 56(8)	0	0
2	2	0	0	0.000 141 960(3)	0.000 042 314(2)	0.000 330 308 5(7)
2	2	1	0	0.000 395 46(6)	0.000 029 093 98(7)	-0.000 267 364(2)
2	2	2	0	0.000 728 681 6(4)	0	0
3	2	0	0	0	0	-0.000 019 835(1)
3	2	1	0	0	0	-0.000 012 492 81(2)

TABLE XI. Contribution of diagrams 12, 13, 19, 20, for the Iwasaki action.

$i$	$e_{12-13}^{(i)}$	$e_{19-20}^{(i)}$
0	0.000 261 920(6)	0.000 173 538(9)
1	-0.000 030 833 9(1)	-0.000 277 17(1)
2	0.000 370 942(2)	0.000 258 332(8)
3	0	-0.000 395 294(3)
4	0	-0.000 077 953 8(3)

TABLE XII. Contribution of diagrams 21–23, 25, 27, 28, for the Iwasaki action.

$i$	$j$	$k$	$e_{21-23}^{(i,j,k)}$	$e_{25}^{(i,j,k)}$	$e_{27}^{(i,j,k)}$	$e_{28}^{(i,j,k)}$
0	0	0	0.000 373 419(3)	-0.000 158 621(4)	-0.000 094 848(3)	-0.000 175 933 6(5)
0	2	0	-0.000 373 419(3)	0.000 079 311(2)	0	0.000 087 966 8(3)
1	0	0	-0.000 887 295(1)	0.000 139 681 9(4)	0.000 045 158(4)	0.000 189 311 3(5)
1	2	0	0.000 887 295(1)	0.000 085 189(2)	0	-0.000 120 480(1)
2	0	0	0.000 194 437(1)	-0.000 031 939 2(3)	0.000 168 506(2)	-0.000 050 926 6(2)
2	2	0	-0.000 194 437(1)	-0.000 005 787(2)	0	0.000 009 875 8(1)
3	0	0	0.000 059 183(3)	0	-0.000 015 234(1)	0
3	2	0	-0.000 059 183(3)	0.000 017 202 2(5)	0	0.000 016 807 2(6)
4	0	0	0.000 006 823 53(1)	0	0.000 007 409 712(6)	0
4	2	0	-0.000 006 823 53(1)	0	0	0

A similar process can be followed for two-loop diagrams. In this case, we set  $N = 3$ ,  $c_2 = 0$  and we use three different values for the flavor number:  $N_f = 0, 2, 3$ . Thus, for the Plaquette, Iwasaki, and DBW2 actions, the total contribution is, respectively:

$$\begin{aligned} N_f = 0: dm_{(2\text{-loop})}^{\text{Plaquette}} &= g^4(-0.125\,562\,6(2) + 0.020\,300\,1(2)c_{\text{SW}} + 0.001\,084\,20(7)c_{\text{SW}}^2 - 0.001\,165\,38(2)c_{\text{SW}}^3 \\ &\quad - 0.000\,099\,672\,5(1)c_{\text{SW}}^4) \end{aligned} \quad (24)$$

$$\begin{aligned} N_f = 2: dm_{(2\text{-loop})}^{\text{Plaquette}} &= g^4(-0.119\,236\,1(2) + 0.017\,387\,0(2)c_{\text{SW}} + 0.008\,364\,98(8)c_{\text{SW}}^2 - 0.004\,857\,27(3)c_{\text{SW}}^3 \\ &\quad - 0.001\,156\,194\,7(4)c_{\text{SW}}^4), \end{aligned} \quad (25)$$

$$\begin{aligned} N_f = 3: dm_{(2\text{-loop})}^{\text{Plaquette}} &= g^4(-0.116\,072\,9(2) + 0.015\,930\,5(2)c_{\text{SW}} + 0.012\,005\,4(1)c_{\text{SW}}^2 - 0.006\,703\,21(3)c_{\text{SW}}^3 \\ &\quad - 0.001\,684\,455\,8(6)c_{\text{SW}}^4), \end{aligned} \quad (26)$$

$$\begin{aligned} N_f = 0: dm_{(2\text{-loop})}^{\text{Iwasaki}} &= g^4(-0.009\,952\,3(2) - 0.002\,430\,4(5)c_{\text{SW}} - 0.002\,328\,55(4)c_{\text{SW}}^2 - 0.000\,321\,00(2)c_{\text{SW}}^3 \\ &\quad - 0.000\,041\,936\,5(1)c_{\text{SW}}^4), \end{aligned} \quad (27)$$

$$\begin{aligned} N_f = 2: dm_{(2\text{-loop})}^{\text{Iwasaki}} &= g^4(-0.007\,629\,9(2) - 0.004\,073\,1(5)c_{\text{SW}} + 0.001\,027\,58(6)c_{\text{SW}}^2 - 0.002\,429\,24(3)c_{\text{SW}}^3 \\ &\quad - 0.000\,457\,690(2)c_{\text{SW}}^4), \end{aligned} \quad (28)$$

$$\begin{aligned} N_f = 3: dm_{(2\text{-loop})}^{\text{Iwasaki}} &= g^4(-0.006\,468\,7(2) - 0.004\,894\,4(5)c_{\text{SW}} + 0.002\,705\,65(7)c_{\text{SW}}^2 - 0.003\,483\,35(3)c_{\text{SW}}^3 \\ &\quad - 0.000\,665\,567(2)c_{\text{SW}}^4), \end{aligned} \quad (29)$$

$$\begin{aligned} N_f = 0: dm_{(2\text{-loop})}^{\text{DBW2}} &= g^4(+0.005\,099(2) - 0.005\,390\,3(7)c_{\text{SW}} - 0.001\,115\,7(1)c_{\text{SW}}^2 - 0.000\,044\,82(2)c_{\text{SW}}^3 \\ &\quad - 0.000\,011\,147\,0(2)c_{\text{SW}}^4), \end{aligned} \quad (30)$$

$$\begin{aligned} N_f = 2: dm_{(2\text{-loop})}^{\text{DBW2}} &= g^4(+0.005\,944(2) - 0.006\,184\,0(7)c_{\text{SW}} + 0.000\,204\,6(2)c_{\text{SW}}^2 - 0.001\,017\,7(3)c_{\text{SW}}^3 \\ &\quad - 0.000\,125\,065(3)c_{\text{SW}}^4), \end{aligned} \quad (31)$$

$$\begin{aligned} N_f = 3: dm_{(2\text{-loop})}^{\text{DBW2}} &= g^4(+0.006\,366(2) - 0.006\,580\,9(7)c_{\text{SW}} + 0.000\,864\,8(2)c_{\text{SW}}^2 - 0.001\,504\,2(4)c_{\text{SW}}^3 \\ &\quad - 0.000\,182\,023(5)c_{\text{SW}}^4). \end{aligned} \quad (32)$$

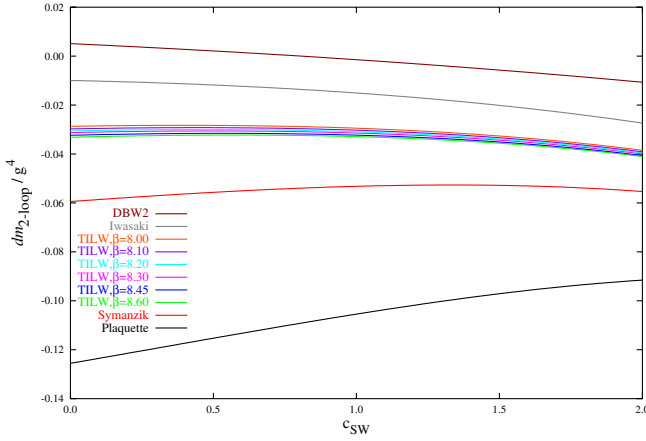


FIG. 3 (color online). Total contribution of two-loop diagrams, for  $N = 3$ ,  $N_f = 0$ , and  $c_2 = 0$ . Legends appear in the same top-to-bottom order as the corresponding lines.

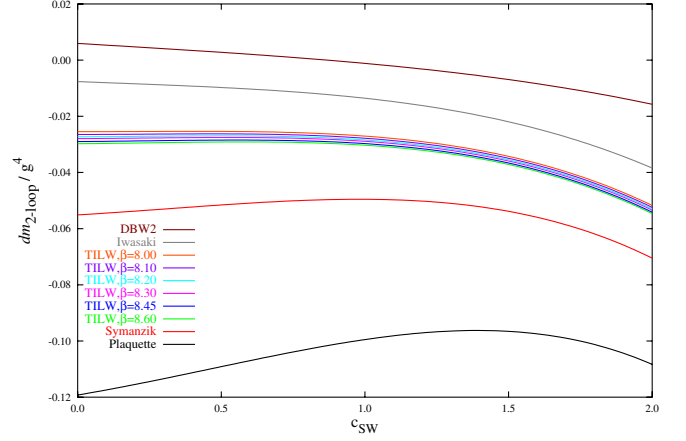


FIG. 4 (color online). Total contribution of two-loop diagrams, for  $N = 3$ ,  $N_f = 2$ , and  $c_2 = 0$ . Legends appear in the same top-to-bottom order as the corresponding lines.

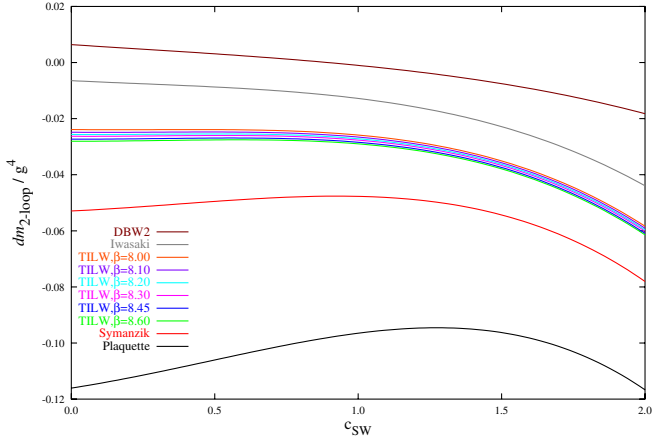


FIG. 5 (color online). Total contribution of two-loop diagrams, for  $N = 3$ ,  $N_f = 3$ , and  $c_2 = 0$ . Legends appear in the same top-to-bottom order as the corresponding lines.

In Figs. 3–5 we present the values of  $dm_{(2\text{-loop})}$  for  $N_f = 0, 2, 3$ , respectively; the results are shown for all choices of Symanzik actions which we have considered, as a function of  $c_{SW}$  ( $N = 3, c_2 = 0$ ). In all cases, the dependence on  $c_{SW}$  is rather mild. One observes that  $dm_{(2\text{-loop})}$  is significantly smaller for all improved actions, as compared to the plaquette action; in particular, in the case of DBW2,  $dm_{(2\text{-loop})}$  is closest to zero and it vanishes exactly around  $c_{SW} = 1$ .

Another feature of these results is that they change only slightly with  $N_f$ , especially in the range  $c_{SW} < 1.5$ . This is due to the small contributions of diagrams with closed fermion loops (diagrams 12, 13, 19, 20). By the same token, in the case of nondegenerate flavors,  $dm_{(2\text{-loop})}$  is expected to depend only weakly on the mass of the virtual fermion.

#### IV. IMPROVED PERTURBATION THEORY

We now apply our method of improving perturbation theory [7–9], based on resummation of an infinite subset of tadpole diagrams, termed “cactus” diagrams. In Ref. [9] we show how this procedure can be applied to any action of the type we are considering here, and it provides a simple, gauge invariant way of dressing, to all orders, perturbative results at any given order (such as the one- and two-loop results of the present calculation). Some alternative ways of improving perturbation theory have been proposed in Refs. [17,18]. In a nutshell, our procedure involves replacing the original values of the Symanzik and clover coefficients by improved values, which are explicitly computed in [9]. Applying at first this method to one-loop diagrams, the improved (“dressed”) value  $dm^{\text{dr}}$  of the critical mass ( $N = 3, c_2 = 0$ ) can be written as

$$dm_{(1\text{-loop})}^{\text{dr}} = \sum_{i=0}^2 \varepsilon_{\text{dr}}^{(i)} c_{SW}^i. \quad (33)$$

In comparing with  $\varepsilon^{(i)}$  of Eq. (20), the quantity  $\varepsilon_{\text{dr}}^{(i)}$  is the result of one-loop Feynman diagrams with dressed values for the Symanzik parameters, and it has already been multiplied by  $g^2(N^2 - 1)/N$ . The dependence of  $\varepsilon_{\text{dr}}^{(i)}$  on  $g$  is quite complicated now, and cannot be given in closed form; instead  $\varepsilon_{\text{dr}}^{(i)}$  must be computed numerically for particular choices of  $g$ . Listed in Table XIII are the results for  $\varepsilon_{\text{dr}}^{(i)}$  along with the value of  $\beta = 2N/g^2$  corresponding to each one of the 16 actions used in this calculation.

An attractive feature of this improvement procedure is that it can be applied also to higher-loop perturbative results, with due care to avoid double counting of the cactus diagrams which were already included at one loop. Ideally, of course, one-loop improvement should al-

TABLE XIII. Results for  $dm_{(1\text{-loop})}^{\text{dr}}$  (Eq. (33)), with  $N = 3$ .

Action	$\beta$	$\varepsilon_{\text{dr}}^{(0)}$	$\varepsilon_{\text{dr}}^{(1)}$	$\varepsilon_{\text{dr}}^{(2)}$
Plaquette	6.00	-0.579 221 119(2)	0.115 954 757 0(3)	0.036 180 677 88(9)
Symanzik	5.00	-0.486 979 757 8(8)	0.112 136 999 9(4)	0.035 386 053 57(4)
Symanzik	5.07	-0.478 756 110(2)	0.110 724 129 96(5)	0.035 072 383 06(5)
Symanzik	6.00	-0.391 522 652 2(2)	0.094 796 200 1(5)	0.031 241 384 29(9)
TILW (8.60)	3.7120	-0.535 877 034 8(7)	0.126 591 763 8(3)	0.038 139 638 51(4)
TILW (8.45)	3.6018	-0.549 741 533 8(3)	0.129 110 464 4(3)	0.038 633 711 3(1)
TILW (8.30)	3.4772	-0.565 140 738 6(9)	0.131 926 376 9(1)	0.039 169 506 9(1)
TILW (8.20)	3.3985	-0.575 611 153 1(9)	0.133 793 755 8(7)	0.039 517 130 46(7)
TILW (8.10)	3.3107	-0.587 012 277 2(4)	0.135 843 782 5(6)	0.039 889 914 3(3)
TILW (8.00)	3.2139	-0.599 415 804(1)	0.138 085 996(2)	0.040 287 713 3(4)
Iwasaki	1.95	-0.757 856 451(1)	0.167 100 781 9(8)	0.044 746 728 234(1)
Iwasaki	2.20	-0.655 510 208 5(5)	0.153 774 819 3(6)	0.042 931 836 56(3)
Iwasaki	2.60	-0.541 348 980(1)	0.135 988 244 0(3)	0.039 676 264 95(6)
DBW2	0.6508	-0.774 994 351 2(7)	0.184 724 488 9(1)	0.047 317 178 66(3)
DBW2	0.8700	-0.574 781 578(1)	0.157 568 840 9(9)	0.042 812 619 80(1)
DBW2	1.0400	-0.482 286 334 3(9)	0.141 249 923 0(5)	0.039 186 543 574(5)

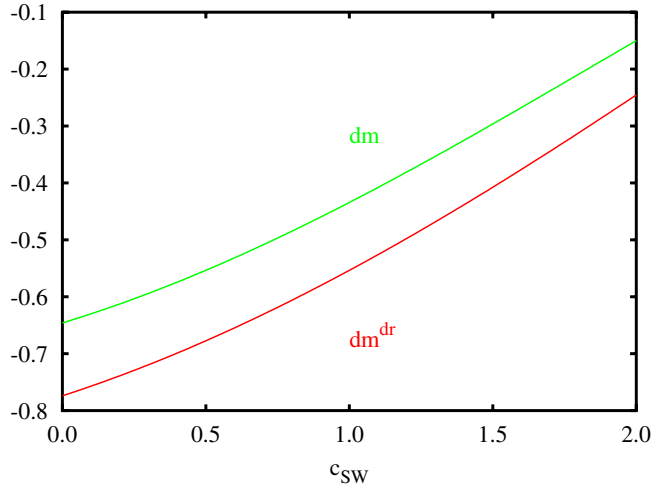


FIG. 6 (color online). Improved and unimproved values of  $dm$  up to two loops, as a function of  $c_{\text{SW}}$ , for the plaquette action ( $\beta = 5.29$ ,  $N = 3$ ,  $N_f = 2$ ).

ready be adequate enough, so as to obviate the need to consider higher loops; indeed, we find this to be the case and, consequently, we limit our discussion of two-loop improvement to only the plaquette action ( $\beta = 5.29$ ,  $N = 3$ ,  $N_f = 2$ ), the Iwasaki action ( $\beta = 1.95$ ,  $N = 3$ ,

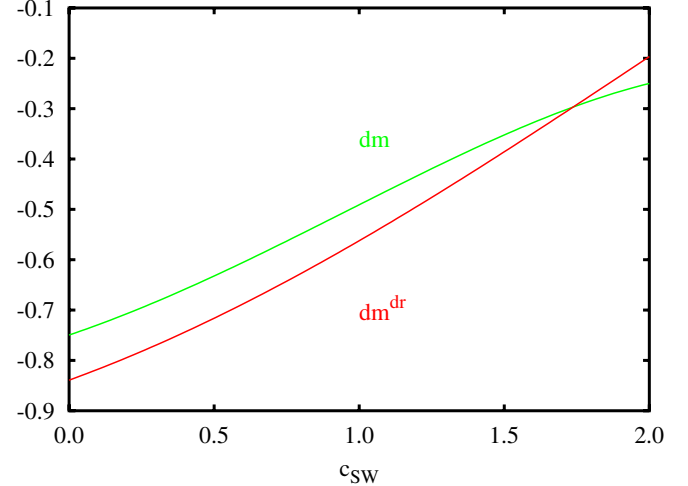


FIG. 7 (color online). Improved and unimproved values of  $dm$  up to two loops, as a function of  $c_{\text{SW}}$ , for the Iwasaki action ( $\beta = 1.95$ ,  $N = 3$ ,  $N_f = 2$ ).

$N_f = 2$ ), and the DBW2 action ( $\beta = 0.87$  and  $\beta = 1.04$ ,  $N = 3$ ,  $N_f = 2$ ). Using these values, the contribution to  $dm_{(2\text{-loop})}^{\text{dr}}$  is a polynomial in  $c_{\text{SW}}$ :

$$\begin{aligned} dm_{(2\text{-loop}), \text{plaquette}}^{\text{dr}} = & -0.77398(8) + 0.16330(4)c_{\text{SW}} + 0.06224534(1)c_{\text{SW}}^2 - 0.0044006(9)c_{\text{SW}}^3 \\ & - 0.00073780(6)c_{\text{SW}}^4, \end{aligned} \quad (34)$$

$$\begin{aligned} dm_{(2\text{-loop}), \text{Iwasaki}}^{\text{dr}} = & -0.0813302(9) + 0.043030(3)c_{\text{SW}} + 0.0308196(2)c_{\text{SW}}^2 - 0.00767090(8)c_{\text{SW}}^3 \\ & - 0.001160923(1)c_{\text{SW}}^4, \end{aligned} \quad (35)$$

$$\begin{aligned} dm_{(2\text{-loop}), \text{DBW2}(\beta=0.87)}^{\text{dr}} = & -0.044906(1) + 0.029449(4)c_{\text{SW}} + 0.0239522(2)c_{\text{SW}}^2 - 0.0082231(1)c_{\text{SW}}^3 \\ & - 0.001218955(4)c_{\text{SW}}^4, \end{aligned} \quad (36)$$

$$\begin{aligned} dm_{(2\text{-loop}), \text{DBW2}(\beta=1.04)}^{\text{dr}} = & -0.031260(1) + 0.021793(2)c_{\text{SW}} + 0.0188027(2)c_{\text{SW}}^2 - 0.00705284(9)c_{\text{SW}}^3 \\ & - 0.001055657(1)c_{\text{SW}}^4. \end{aligned} \quad (37)$$

The comparison between the total dressed contribution  $dm^{\text{dr}} = dm_{(1\text{-loop})}^{\text{dr}} + dm_{(2\text{-loop})}^{\text{dr}}$  and the unimproved contribution,  $dm$ , for the plaquette action is exhibited in Fig. 6, as a function of  $c_{\text{SW}}$ . Similarly,  $dm^{\text{dr}}$  for the Iwasaki and the DBW2 actions is shown in Figs. 7 and 8, respectively.

Finally, in Table XIV, we present a comparison of dressed and undressed results, for some commonly used values of  $\beta$ ,  $N_f$ ,  $c_{\text{SW}}$ , and we also compare with available nonperturbative estimates for  $\kappa_c$  [10,19–22]. We observe that improved perturbation theory, applied to one-loop results, already leads to a much better agreement with the nonperturbative estimates.

## V. DISCUSSION

To recapitulate, in this paper we have calculated the critical mass  $m_c$ , and the associated critical hopping parameter  $\kappa_c$ , up to two loops in perturbation theory, using the clover action for fermions and the Symanzik improved gluon action with 4- and 6-link loops. The perturbative value of  $m_c$  is a necessary ingredient in the higher-loop renormalization of operators, in mass independent schemes: Such renormalizations are typically defined and calculated at vanishing renormalized mass, which amounts to setting the Lagrangian mass equal to  $m_c$ .

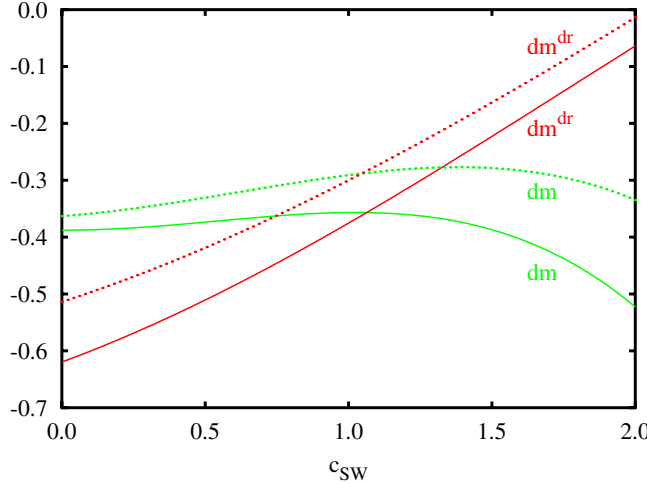


FIG. 8 (color online). Improved and unimproved values of  $dm$  up to two loops, as a function of  $c_{SW}$ , for the DBW2 action ( $N = 3$ ,  $N_f = 2$ ). We set  $\beta = 0.87$  (solid lines) and  $\beta = 1.04$  (dotted lines).

In our calculations, we have chosen for the Symanzik coefficients  $c_i$  a wide range of values, which are most commonly used in numerical simulations. The dependence of our results on the number of colors  $N$  and the number of fermion flavors  $N_f$  is shown explicitly. The dependence on the clover parameter  $c_{SW}$  is in the form of a fourth degree polynomial whose coefficients we compute explicitly; it is expected, of course, that the most relevant values for  $c_{SW}$  are those optimized for  $\mathcal{O}(a)$  improvement, either at tree level ( $c_{SW} = 1$ ), or at one loop [1], or nonperturbatively [10].

Since  $m_c$  is gauge invariant, we chose to calculate it in the Feynman gauge. The propagator appearing in Feynman diagrams is the inverse of a nondiagonal matrix; while this inverse can be written down explicitly, it is more convenient, and more efficient in terms of CPU time, to perform the inversion numerically. Integrations over loop momenta

were performed as momentum sums on lattices of finite size  $L$ , where typically  $L \lesssim 40$ ; extrapolation to  $L \rightarrow \infty$  introduces a systematic error, which we estimate quite accurately.

Our results for  $m_c$  are significantly closer to zero in the case of Symanzik improved actions, as compared to the plaquette action. In particular, the DBW2 action stands out among the rest, in that  $m_c$  vanishes exactly for a value of  $c_{SW}$  around 1. Thus, improved actions seem to bring us quite near the point of chiral symmetry restoration. The dependence of  $m_c$  on the number of flavors is seen to be very mild. This fact would also suggest that, in the case of nondegenerate flavors,  $m_c$  should depend only weakly on the mass of the virtual fermion.

Finally, we have made some comparisons among perturbative and nonperturbative results for  $\kappa_c$ . While these are expected to differ for a power divergent additive renormalization, such as the quantity under study, we nevertheless find a reasonable agreement. This agreement is further enhanced upon using an improved perturbative scheme, which entails resumming, to all orders in the coupling constant, a dominant subclass of tadpole diagrams. The method, originally proposed for the Plaquette action (see Ref. [7]), was extended in Ref. [9] to encompass all possible gluon actions made of closed Wilson loops, and can be applied at any given order in perturbation theory. As would be desirable, one-loop improvement is seen to be already adequate to give a reasonable agreement among perturbative and nonperturbative values. Indeed, our results for  $\kappa_{1\text{-loop}}^{\text{dr}}$  are significantly closer to the nonperturbative evaluations, as shown in Table XIV; in fact, the two-loop dressing procedure introduces no further improvement to the comparison.

## ACKNOWLEDGMENTS

This work is supported in part by the Research Promotion Foundation of Cyprus (Proposal No. ENTAΞ/0504/11 and No. ENΙΣΧ/0505/45).

TABLE XIV. One- and two-loop results, and nonperturbative estimates for  $\kappa_c$ .

Action	$N_f$	$\beta$	$c_{SW}$	$\kappa_{1\text{-loop}}$	$\kappa_{2\text{-loop}}$	$\kappa_{1\text{-loop}}^{\text{dr}}$	$\kappa_{2\text{-loop}}^{\text{dr}}$	$\kappa_c^{\text{non-pert}}$ [Ref.]
Plaquette	0	6.00	1.479	0.1301	0.1335	0.1362	0.1362	0.1392 [19]
Plaquette	0	6.00	1.769	0.1275	0.1306	0.1337	0.1332	0.1352 [10]
Plaquette	2	5.29	1.9192	0.1262	0.1307	0.1353	0.1341	0.1373 [20]
Iwasaki	2	1.95	1.53	0.1292	0.1368	0.1388	0.1379	0.1421 [22]
TILW (8.60)	0	3.7120	1.0	0.1339	0.1370	0.1378	0.1384	
TILW (8.00)	0	3.2139	1.0	0.1348	0.1387	0.1397	0.1406	
DBW2	2	0.87	0.0	0.1502	0.1384	0.1460	0.1479	
DBW2	2	0.87	1.0	0.1352	0.1372	0.1379	0.1379	
DBW2	2	1.04	0.0	0.1454	0.1375	0.1421	0.1434	
DBW2	2	1.04	1.0	0.1334	0.1348	0.1352	0.1352	

- [1] B. Sheikholeslami and R. Wohlert, Nucl. Phys. **B259**, 572 (1985).
- [2] K. Symanzik, Nucl. Phys. **B226**, 187 (1983); **B226**, 205 (1983).
- [3] A. Skouroupathis and H. Panagopoulos, Phys. Rev. D **76**, 094514 (2007).
- [4] E. Follana and H. Panagopoulos, Phys. Rev. D **63**, 017501 (2000).
- [5] H. Panagopoulos and Y. Proestos, Phys. Rev. D **65**, 014511 (2001).
- [6] S. Caracciolo, A. Pelissetto, and A. Rago, Phys. Rev. D **64**, 094506 (2001).
- [7] H. Panagopoulos and E. Vicari, Phys. Rev. D **58**, 114501 (1998).
- [8] H. Panagopoulos and E. Vicari, Phys. Rev. D **59**, 057503 (1999).
- [9] M. Constantinou, H. Panagopoulos, and A. Skouroupathis, Phys. Rev. D **74**, 074503 (2006).
- [10] M. Lüscher *et al.*, Nucl. Phys. **B491**, 323 (1997).
- [11] M. Lüscher and P. Weisz, Phys. Lett. B **158**, 250 (1985).
- [12] Y. Iwasaki, University of Tsukuba Report No. UTHEP-118, 1983.
- [13] K. Symanzik, Nucl. Phys. **B226**, 187 (1983).
- [14] M. Lüscher and P. Weisz, Commun. Math. Phys. **97**, 59 (1985); **98**, 433(E) (1985).
- [15] M. G. Alford *et al.*, Phys. Lett. B **361**, 87 (1995).
- [16] T. Takaishi, Phys. Rev. D **54**, 1050 (1996).
- [17] G. Parisi, in *Proceedings of the 20th International Conference on High Energy Physics, Madison, 1980*, edited by L. Durand and L. G. Pondrom (AIP, New York, 1981).
- [18] G. P. Lepage and P. B. Mackenzie, Phys. Rev. D **48**, 2250 (1993).
- [19] K. C. Bowler *et al.* (UKQCD Collaboration), Phys. Rev. D **62**, 054506 (2000).
- [20] C. R. Allton *et al.* (UKQCD Collaboration), Phys. Rev. D **65**, 054502 (2002).
- [21] M. Della Morte *et al.* (ALPHA Collaboration), J. High Energy Phys. 07 (2005) 007.
- [22] A. Ali Khan *et al.* (CP-PACS Collaboration), Phys. Rev. D **65**, 054505 (2002); **67**, 059901(E) (2003).